Long-Term LoRa Experiments in a Chemical Plant

Jessica Breitegger*, Christian Raffelsberger*, Siddhartha S. Borkotoky‡*,
Ingomar Rogler§, and Christian Bettstetter*†

*Lakeside Labs GmbH, 9020 Klagenfurt, Austria
†University of Klagenfurt, Institute of Networked and Embedded Systems, 9020 Klagenfurt, Austria
‡ Indian Institute of Technology Bhubaneswar, Khordha 752050, India
§Treibacher Industrie AG, 9330 Althofen, Austria

***Abstract*—We report on multi-month experiments of a LoRa network deployed in a chemical plant. Using measurement data of nodes distributed (*i*) inside a building and (*ii*) over multiple buildings, all sending to a gateway, we estimate the path loss and fading characteristics of the links. Although we operate the system in a harsh environment according to these measurements — with a path loss exponent up to 5.1 and Nakagami fading with m as low as 0.7 — the packet loss rate is low for in-building links (2.5 % on the average), demonstrating LoRa's suitability for certain industrial applications.**

***Index Terms*—industrial sensor networks, LoRa, LoRaWAN, path loss, fading**

I. Introduction

Low-power wide-area networks (LPWAN) enable low-rate wireless connectivity to energy-limited devices spread over large areas [1]. Various technologies have been developed for this purpose — including DASH7, Sigfox, and LoRa — and industries deploy them to optimize production and maintenance [2], [3]. In such an industrial context, namely in a chemical plant, we conduct experiments over several months using LoRaWAN Class A sensors. The system is a multipoint-to-point network with sensors periodically sending measurements to a LoRaWAN gateway. Our contributions are to model the radio channel and study the packet losses based on these long-term real-world measurements. Using standard and flexible models for path loss and fading, we find the model parameters that best match this industrial environment. Such parametrization is useful for the design and setup of LoRaWANs in the industry. Moreover, the analysis of the parameter setting in harsh industrial radio environments could be of interest to fellow researchers and network designers.

The paper is organized as follows: Section II addresses related work. Section III presents the models for small-scale fading, path loss, and packet loss ratio. Section IV explains the measurement setups: an intra-building scenario (see Fig. 1) and an inter-building scenario. Sections V and VI present the results and their interpretation. Finally, Section VII concludes.

II. Related Work

There are many studies on empirical channel models and experimental performance analysis in industrial indoor environments. They use channel sounders [4] or specific technologies, like IEEE 802.11ax [5] and 802.15.4 [6]. In the narrower context of the LoRa physical layer and LoRaWAN, it was studied how well LoRaWAN is suited for indoor industrial monitoring and how network parameters should be set [7]. A channel hopping scheme to improve the performance in industrial applications was proposed [8]; the coverage and performance in an indoor market environment was assessed in terms of RSSI and SNR [9]; and the coverage in urban and rural areas was studied for different communication ranges and spreading factors [10]. In contrast to the work in this paper, those papers do not cover channel modeling. An experimental evaluation of NB-IoT and LoRaWAN for industrial applications is given in [11]. The evaluation focuses on energy efficiency and shows that LoRaWAN is up to 10 times more efficient than NB-IoT, especially for small message payloads. A channel attenuation model for LoRa based on real-world measurements was proposed for outdoor environments [12]. However, the evaluated outdoor environments differ significantly and hence the models are not applicable for a chemical plant.

This work has been supported by the K-project DeSSnet (Dependable, secure and time-aware sensor networks), which is funded within the context of COMET – Competence Centers for Excellent Technologies by the Austrian Ministry for Transport, Innovation and Technology (BMVIT), the Federal Ministry for Digital and Economic Affairs (BMDW), and the federal states of Styria and Carinthia; the COMET program is conducted by the Austrian Research Promotion Agency (FFG).

Fig. 1: Hall in a chemical plant: view from the ground floor

III. Channel Modeling and Evaluation Metrics

A. Small-Scale Fading

A common and versatile approach to describe small-scale fading is the Nakagami-m model with $m \geq 1/2$ describing the severity of fading. The instantaneous reception power p_r in watts is gamma distributed: $p_r \sim \Gamma(k, \theta)$.

We parameterize Nakagami fading for our environment using measurements of the RSSI as an indicator for p_r. Our hypothesis is that the square root of the linear RSSI values has a Nakagami(m,Ω) probability density function (pdf),

$$f(x;m,\Omega) = \frac{2m^m}{\Gamma(m)\,\Omega^m}\, x^{2m-1} \exp\left(-\frac{m}{\Omega}x^2\right), \qquad (1)$$

with parameters m and $\Omega > 0$. Our approach is to fit *normalized* RSSI values, i.e., we first remove the effects of path loss and shadowing for each sensor. In particular, we subtract the mean RSSI of a given sensor (computed in the linear domain) from every single RSSI measurement: $\Delta\text{RSSI}^{(\text{dB})} = \text{RSSI}^{(\text{dBm})} - \overline{\text{RSSI}}^{(\text{dBm})}$. To get the parameters m and Ω, we first fit the linear ΔRSSI to a gamma distribution and set $m = k$ and $\Omega = \frac{\theta}{m}$.

B. Path Loss

The path loss is modeled by

$$\overline{p_r}^{(\text{dBm})} = p_t^{(\text{dBm})} + K^{(\text{dB})} - 10\alpha \log_{10}\left(\frac{d}{d_0}\right) \text{dB}, \qquad (2)$$

where $\overline{p_r}$ is the mean reception power ($\overline{\text{RSSI}}$ in our case), p_t is the transmission power, α is the path loss exponent, d is the distance between sender (sensors) and receiver (gateway), d_0 is a reference distance, and $K^{(\text{dB})} = -20\log_{10}(4\pi d_0/\lambda)\,\text{dB}$ is a dimensionless constant with wavelength $\lambda = \frac{c}{f}$ with speed of light c and radio frequency f. We use f to be the mean value of the carrier frequencies over all channels. To determine the distances d, we use floor plans of the plant and manually measure the distances between the sensors and the gateway. Algorithms for node localization [13] could also be used.

Our objective is to find the α that minimizes the mean squared error (MSE) between the path loss model (2) and the actual $\overline{\text{RSSI}}$ values using the methodology explained in [14]. The MSE is defined by:

$$\text{MSE}(\alpha) = \frac{1}{n}\sum_{i=1}^{n}\left[\overline{\text{RSSI}}^{(\text{dBm})}(d_i) - \widehat{\overline{\text{RSSI}}}^{(\text{dBm})}(d_i)\right]^2, \qquad (3)$$

where n is the total number of sensors, $\overline{\text{RSSI}}(d_i)$ is the mean RSSI value at distance d_i from measurements and $\widehat{\overline{\text{RSSI}}}(d_i)$ is the mean RSSI value estimated by the model at this distance.

C. Packet Loss Ratio

We use the packet loss ratio (PLR) to evaluate the performance of LoRa in terms of link reliability. Each sensor includes a sequence number in the message header. We calculate the PLR for each sensor by dividing the number of received packets by the maximum sequence number (counter overflows are taken into account). Based on gaps in the received sequence number pattern, it is also possible to identify the packet loss pattern.

IV. Environment and Measurement Setup

The measurements are conducted at a production site of a chemical plant. The environment is characterized by heavy machinery, pipes, and other metallic constructions. The intra-building measurements use nine LoRaWAN class A nodes (battery-powered nke Watteco Press'O and Sense'O sensors), placed along a chain conveyor spanning several floors (Fig. 1). The LoRaWAN gateway (MultiTech Conduit) is positioned

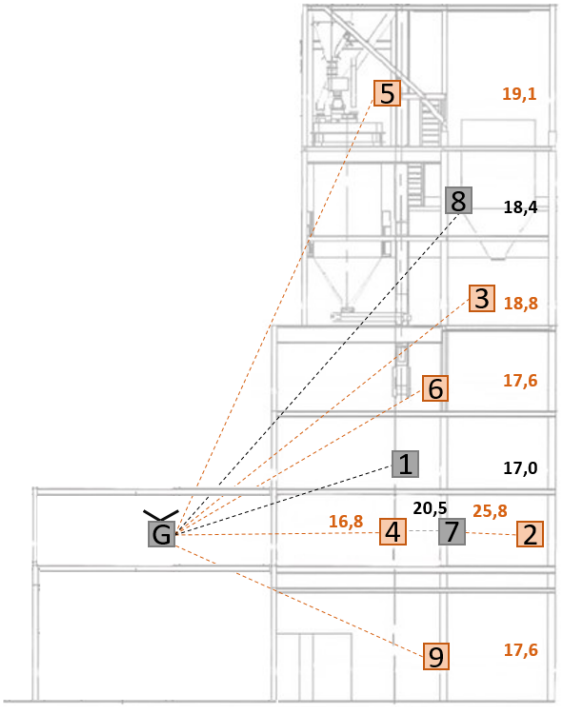

Fig. 2: Floor plan of scenario 1 with distances (in m) between sensors (1 to 9) and gateway (G)

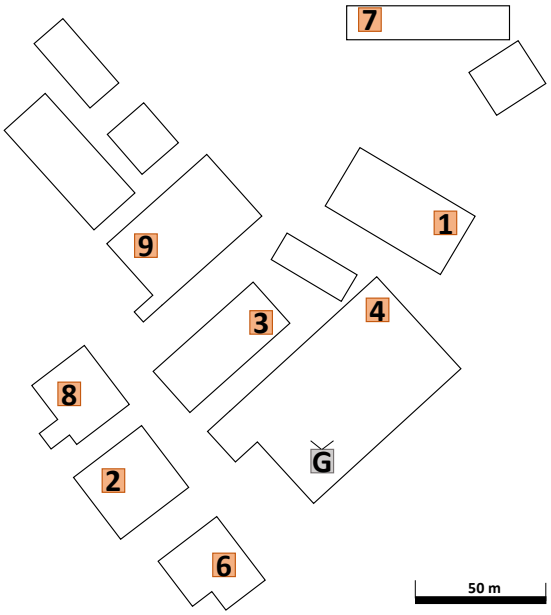

Fig. 3: Deployment plan of scenario 2 with sensors (1 to 8) and gateway (G) located in different buildings

in an adjacent control room separated by a steel wall (scenario 1a). Measurement data is collected over the course of 23 weeks. To evaluate the performance for larger transmission ranges, we relocate the gateway to a different building, roughly 60 m away from the sensors (scenario 1b), and collect data for another 16 weeks. If not noted otherwise, the results for sce-

TABLE I: LoRa configuration parameters

Parameter	Value
Spreading factor	8 to 12
Channel coding rate	4/5
Payload size	11 byte
Channels	1 to 8 (avg. 869 MHz)
Transmission power	14 dBm
Receiver gain	3 dB
Sender gain	0 dB

TABLE II: Sending intervals in minutes

Sensor	Scenario 1	Scenario 2
1	1440	30
2	60	60
3	60	360
4	60	1440
5	60	-
6	60	360
7	1440	10
8	1440	1
9	60	60

nario 1 are from scenario 1a. The inter-building measurements (scenario 2) last for 17 weeks and employ eight LoRaWAN nodes of the same type deployed in different buildings on the site. The distances from the sensors to the gateway range from 57 m to 167 m. All measurements are conducted one after the other. Figs. 2 and 3 show the placement of the sensors and gateway in scenario 1 and 2, respectively.

Table I lists configuration parameters of the transceivers. Table II shows the sending intervals of the sensors. The message length is 24 byte, which consists of a 13-byte header and an 11-byte payload [15]. The gateway logs all received messages, including metadata, such as timestamp, received signal strength indicator (RSSI), signal-to-noise ratio (SNR), channel number, and spreading factor.

V. Evaluation of the Intra-Building Scenario

A. Small-Scale Fading

We analyze the RSSI values for each of the hourly-sending sensors. Table III lists the obtained Nakagami parameters of all sensor links. For scenario 1a, we find that all links have similar fading with a similar MSE. The most severe fading is observed for sensor 3 ($m = 0.70$), the weakest fading for sensor 5 ($m = 0.83$). Fig. 4 shows the histogram of $\sqrt{\Delta\text{RSSI}}$, which represents the channel gain of the signal amplitude, and the estimated Nakagami pdf for sensor 3. The average value of the fading severity over all sensors is $\overline{m} = 0.76$ with an average MSE of $\overline{\text{MSE}} = 0.80$. Recall that Nakagami fading with $m = 1$ corresponds to Rayleigh fading, so the fading in this industrial environment is more severe than Rayleigh fading.

A similar analysis is performed with the gateway located in a different building roughly 60 m away from the sensor nodes on average (scenario 1b). Apart from sensor 2, the severity of the fading has not changed significantly. However, the MSE of the Nakagami model increased in most cases. The mean value is now $\overline{m} = 0.96$ with $\overline{\text{MSE}} = 1.88$.

TABLE III: Parameter m and MSE of the Nakagami-m fitting

(a) Scenario 1a

Sensor	m	MSE
2	0.74	0.94
3	0.70	0.77
4	0.74	0.74
5	0.83	0.83
6	0.76	0.80
9	0.78	0.72

(b) Scenario 1b

Sensor	m	MSE
2	1.38	3.09
3	0.86	1.86
4	0.90	1.21
5	0.98	0.83
6	0.89	2.86
9	0.77	1.41

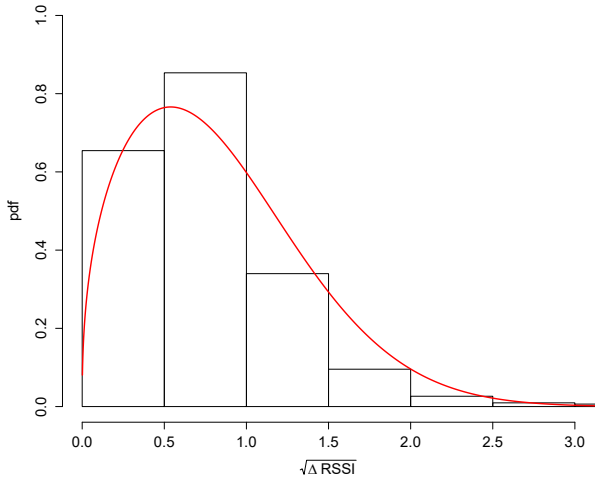

Fig. 4: Histogram showing the channel gain of the signal amplitude $\sqrt{\Delta\text{RSSI}}$ and the estimated Nakagami-m pdf

Fig. 5 shows the Nakagami pdfs for scenario 1a and scenario 1b for several sensor links. Our basic observation is that the pdfs are more homogeneous for scenario 1a than for scenario 1b. The general fading behavior is similar.

B. Path Loss

After the analysis of small-scale fading, we model the path loss for scenario 1a. Table IVa shows i.a. the mean RSSI values and the distances of each sensor to the gateway required for the calculation according to (2). Testing all integer values of d_0 from 1 to 10 meters, we find that $d_0 = 1$ m yields the α with the lowest MSE. Using $d_0 = 1$ m and $f = 869$ MHz yields $K = -31.23$ dB. Substituting K, the sending and received power, and the distances in (3) with the values from Table IVa, we get $\text{MSE}(\alpha) = 38810 - 15061\alpha + 1469\alpha^2$. Differentiating $\text{MSE}(\alpha)$ relative to α and setting it to zero yields $\alpha = 5.13$ with a MSE of about 23 dB^2.

Fig. 6 shows all RSSI measurements and their mean for a given distance along with the resulting path loss model.

C. Packet Loss Ratio

Table IVa contains i.a. the packet statistics for scenario 1a, including the number of sent and lost packets, the PLR, and the RSSI and SNR values. The overall loss rate of the sensors is 2.5 %. The PLR is highest for the sensors with the lowest RSSI and SNR mean values. Table IVb shows the packet

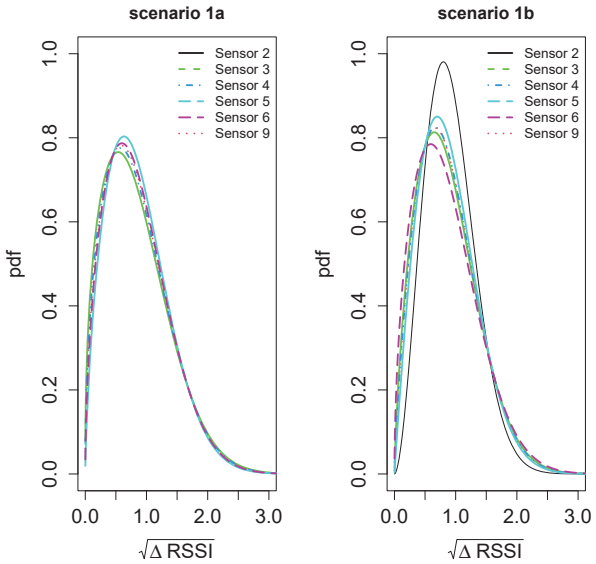

Fig. 5: Nakagami probability density functions of sensor links (scenario 1)

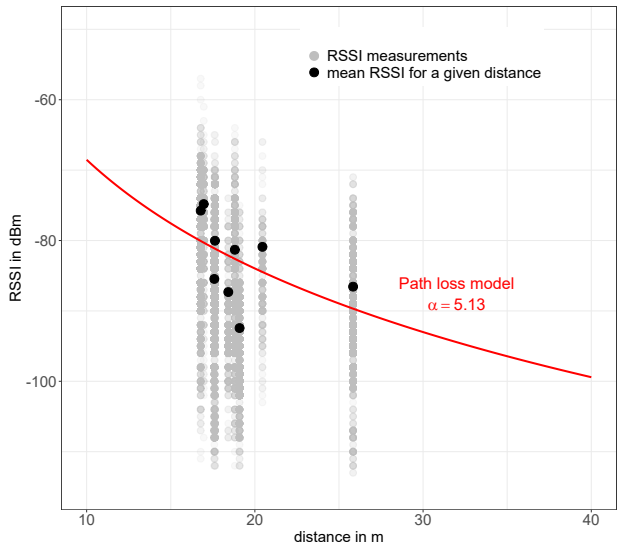

Fig. 6: RSSI measurements, mean RSSI, and path loss model (scenario 1)

statistics for scenario 1b. It is important to note that all sensors used a fixed spreading factor SF8 for all uplink transmissions. Thus, the RSSI and SNR values for all sensors have dropped severely compared to scenario 1a. This also results in an overall increased PLR of 19.8 %. The high loss rate is mainly caused by two sensors (sensor 2 and 6) with a PLR of nearly 60 %. For these sensors, the $\overline{\text{RSSI}}$ is -104 dBm and the received signal power is below the noise level (negative $\overline{\text{SNR}}$).

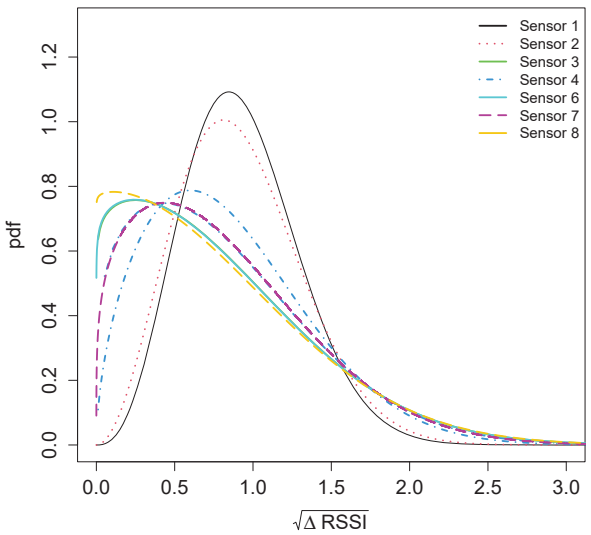

Fig. 7: Nakagami probability density functions of sensor links (scenario 2)

VI. Evaluation of the Inter-Building Scenario

A. Small-Scale Fading

Using the methodology described in Section III-A and assuming Nakagami fading to be the appropriate fading distribution in the considered environment, we analyze the RSSI values for each sensor. The analysis shows that the measurement data of all of the eight sensors already provide valid Nakagami-m-parameters. Figure 7 shows the Nakagami pdfs of the sensors. Table V lists the Nakagami parameters of all sensor links for scenario 2. Observing Table V, we find that the links do not have similar fading but have comparable MSE. The most severe fading is observed for sensor 9 ($m = 0.51$), the weakest for sensor 2 ($m = 1.41$).

B. Path Loss

After the analysis of the fading, we also aim to model the path loss for scenario 2. Using the methodology of Section III-B, Table IVc shows i.a. the mean RSSI values and the distances of each sensor to the gateway required for the calculation. Referencing to (3), we get a path loss exponent $\alpha = 4.2$, which means that although the path loss is still high, it is lower for the inter-building scenario than for the intra-building scenario (scenario 1) with $\alpha = 5.1$.

C. Packet Loss Ratio

For this scenario, we enable the adaptive data rate (ADR) mechanism, where the LoRaWAN gateway instructs the nodes to change the spreading factor (SF) based on the RSSI. Due to larger distances and obstacles between the nodes and the gateway, most sensors send with SF12, but we also observe SF switching when the channel conditions change. Table VI includes the number of packets received with different spreading factors. Even though SF12 is used for most sensors, some of them experience a high packet loss. The high packet loss of sensors 1, 2, 4, and 8 can be attributed to the low RSSI and

TABLE IV: Packet statistics

(a) Scenario 1a: All sensors are in one hall, gateway is in an adjacent control room

Sensor	S1	S2	S3	S4	S5	S6	S7	S8	S9
Packets sent	489	3977	3982	3982	3982	3982	329	489	3981
Packets received	478	3884	3948	3955	3723	3926	317	469	3948
PLR (%)	2.25	2.34	0.85	0.68	6.50	1.41	3.65	4.09	0.83
$\overline{\text{SNR}}$ (dB)	10.1	6.9	8.9	9.9	2.6	7.5	8.8	5.9	9.1
$\sigma(\text{SNR})$ (dB)	1.6	2.9	2.0	1.6	4.6	2.5	2.1	4.0	1.9
$\overline{\text{RSSI}}$ (dBm)	−74.8	−86.6	−81.3	−75.8	−92.4	−85.5	−80.9	−87.4	−80.0
$\sigma(\text{RSSI})$ (dBm)	7.3	9.7	10.4	9.0	12.7	11.9	12.6	10.1	6.5
Distance (m)	17.0	25.8	18.8	16.8	19.1	17.6	20.5	18.4	17.6

(b) Scenario 1b: All sensors are in one hall, gateway is in an adjacent building.

Sensors	S1	S2	S3	S4	S5	S6	S7	S8	S9
Packets received	294	1149	2502	1492	478	1107	183	282	2373
Packets sent	314	2627	2627	1530	581[1]	2626	209	314	2627
PLR (%)	6.4	56.3	4.8	2.5	17.7	57.8	12.4	10.2	9.7
$\overline{\text{SNR}}$ (dB)	2.6	−5.5	4.1	4.9	3.2	−4.8	1.5	1.3	1.3
$\sigma(\text{SNR})$ (dB)	4.3	7.1	4.1	3.2	2.4	10.2	5.6	3.6	4.2
$\overline{\text{RSSI}}$ (dBm)	−95.4	−104.5	−96.5	−94.6	−91.9	−103.8	−98.9	−100.7	−98.9
$\sigma(\text{RSSI})$ (dBm)	28.8	11.3	10.3	13.4	3.8	19.3	19.3	3.5	24.3

[1] Sensor 5 experienced a hardware failure after 17 days.

(c) Scenario 2: All sensors and the gateway are located in different buildings.

Sensor	S1	S2	S3	S4	S6	S7	S8	S9
Packets sent	5800	2902	587	357	587	24286	167169	2902
Packets received	2869	1923	563	295	585	21923	130330	2529
PLR (%)	50.5	33.7	4.1	17.4	0.3	9.7	22.0	12.8
$\overline{\text{SNR}}$ (dB)	−14.8	−11.8	1.2	−5.9	8.3	−4.0	−4.1	0.2
$\sigma(\text{SNR})$ (dB)	3.35	3.9	3.8	4.4	2.3	4.5	4.6	4.2
$\overline{\text{RSSI}}$ (dBm)	−105.9	−105.6	−95.8	−101.2	−84.3	−99.6	−100.9	−96.4
$\sigma(\text{RSSI})$ (dBm)	7.1	6.8	14.0	15.4	9.4	17.8	15.6	20.4
Distance (m)	100.7	84.6	57.6	62.6	58.0	167.6	100.8	112.8

TABLE V: Nakagami-m parameter and MSE (scenario 2)

Sensor	m	MSE
1	1.38	0.79
2	1.41	0.74
3	0.53	0.81
4	0.64	0.78
6	0.81	0.79
7	0.54	0.82
8	0.64	0.75
9	0.51	0.80

TABLE VI: Received packets per SF (scenario 2)

Sensor	SF8	SF9	SF10	SF11	SF12
S1	0	0	0	0	2861
S2	0	0	0	0	1923
S3	91	0	0	0	472
S4	0	0	0	0	295
S6	578	0	0	0	7
S7	0	0	0	0	21923
S8	20054	5899	42	4806	99529
S9	1486	0	0	0	1043

SNR mean values. The packet loss rate varies between 0.3% (S6) and 50.5% (S1).

VII. Conclusions

Collecting measurements over several months, we investigated the channel characteristics and PLR of a LoRaWAN deployment in a chemical plant. The fading of the received RSSI values can be appropriately described by the Nakagami-m model. Empirical Nakagami parameters of $m \approx 0.76$ and $m \approx 0.81$ for intra- and inter-building measurements, respectively — in combination with path loss exponents of $\alpha \approx 5.1$ and $\alpha \approx 4.2$, respectively — show that the plant is a harsh environment with multipath propagation and significant attenuation caused by engines, walls, and other metallic objects along with moving obstacles and workers. Despite this environment, the PLR was relatively low with an average of 2.5% for distances up to 26 meters inside the building. Attributed to low RSSI and SNR values, the PLR for some of the sensors raised when the gateway was relocated to another building and for the inter-building scenario. Based on these experiments, it

can be stated that LoRaWAN provides a reasonable solution for industrial wireless sensor networks, especially in the intra-building application considered.

Our deployment covered small-scale LoRaWAN networks. It would be interesting to see how LoRaWAN scales for other industrial applications, requiring more sensors, possibly also with lower sending intervals.

REFERENCES

[1] U. Raza, P. Kulkarni, and M. Sooriyabandara, "Low power wide area networks: An overview," *IEEE Communications Surveys and Tutorials*, vol. 19, no. 2, pp. 855–873, 2017.

[2] V. Gungor and G. Hancke, "Industrial wireless sensor networks: Challenges, design principles, and technical approaches," *IEEE Transactions on Industrial Electronics*, vol. 56, pp. 4258 – 4265, 2009.

[3] A. S., K. Ovsthus, and L. Kristensen, "An industrial perspective on wireless sensor networks — a survey of requirements, protocols, and challenges," *IEEE Communications Surveys & Tutorials*, vol. 16, no. 3, pp. 1391–1412, 2014.

[4] K. Zhang, L. Liu, C. Tao, K. Zhang, Z. Yuan, and J. Zhang, "Wireless channel measurement and modeling in industrial environments," *Advances in Science, Technology and Engineering Systems Journal*, vol. 3, pp. 254–259, 2018.

[5] A. Trassl, T. Hoessler, L. Scheuvens, N. Franchi, and G. Fettweis, "Deriving an empirical channel model for wireless industrial indoor communications," in *Proc. IEEE International Symposium on Personal, Indoor and Mobile Radio Communications (PIMRC)*, 2019, pp. 1–7.

[6] M. Cheffena, "Industrial wireless sensor networks: Channel modeling and performance evaluation," *EURASIP Journal on Wireless Communications and Networking*, vol. 2012, pp. 1–8, 2012.

[7] M. Luvisotto, F. Tramarin, L. Vangelista, and S. Vitturi, "On the use of LoRaWAN for indoor industrial IoT applications," *Wireless Communications and Mobile Computing*, vol. 2018, pp. 1–11, 2018.

[8] M. Rizzi, P. Ferrari, A. Flammini, E. Sisinni, and M. Gidlund, "Using LoRa for industrial wireless networks," in *Proc. IEEE International Workshop on Factory Communication Systems (WFCS)*, 2017.

[9] J. Haxhibeqiri, A. Karaagac, F. Van den Abeele, W. Joseph, I. Moerman, and J. Hoebeke, "LoRa indoor coverage and performance in an industrial environment: Case study," in *Proc. IEEE International Conference on Emerging Technologies and Factory Automation (ETFA)*, 2017, pp. 1–8.

[10] C. Garrido-Hidalgo, T. Olivares, F. J. Ramirez, and L. Roda-Sanchez, "An end-to-end internet of things solution for reverse supply chain management in industry 4.0," *Computers in Industry*, vol. 112, p. 103127, 2019.

[11] M. Ballerini, T. Polonelli, D. Brunelli, M. Magno, and L. Benini, "NB-IoT versus LoRaWAN: An experimental evaluation for industrial applications," *IEEE Transactions on Industrial Informatics*, vol. 16, no. 12, pp. 7802–7811, 2020.

[12] J. Petajajarvi, M. Pettissalo, K. Mikhaylov, A. Roivainen, and T. Hänninen, "On the coverage of LPWANs: Range evaluation and channel attenuation model for LoRa technology," in *Proc. International Conference on ITS Telecommunications (ITST)*, 2015, pp. 55–59.

[13] J. Du, J.-F. Diouris, and Y. Wang, "A RSSI-based parameter tracking strategy for constrained position localization," *EURASIP Journal on Advances in Signal Processing*, vol. 77, no. 1, pp. 1–10, 2017.

[14] A. Goldsmith, *Wireless Communications*. Cambridge University Press, 2004.

[15] "nke Watteco Press'O LoraWAN class A sensor user manual," http://support.nke-watteco.com/presso-2/, accessed: 2020-02-05.